Eliashberg theory with ab-initio Coulomb interactions: a minimal numerical scheme applied to layered superconductors

IOP Publishing J. Phys. Mater. 5 (2022) 024007 https://doi.org/10.1088/2515-7639/ac6041

Journal of Physics: Materials

OPEN ACCESS

RECEIVED
14 January 2022

REVISED
21 March 2022

ACCEPTED FOR PUBLICATION
23 March 2022

PUBLISHED
11 April 2022

PAPER

Eliashberg theory with ab-initio Coulomb interactions: a minimal numerical scheme applied to layered superconductors

Camilla Pellegrini[1], **Rolf Heid**[2] **and Antonio Sanna**[3,*]

[1] Dipartimento di Fisica e Geologia, Universitá degli studi di Perugia, Via Pascoli 33, 06123 Perugia, Italy
[2] Institute for Quantum Materials and Technologies, Karlsruhe Institute of Technology, 76021 Karlsruhe, Germany
[3] Max-Planck-Institut für Mikrostrukturphysik, Weinberg 2, D-06120 Halle, Germany
[*] Author to whom any correspondence should be addressed.

E-mail: sanna@mpi-halle.mpg.de

Keywords: Eliashberg, Coulomb interactions, 2D superconductors

Abstract

We present a minimal approach to include static Coulomb interactions in Eliashberg theory of superconductivity from first principles. The method can be easily implemented in any existing Eliashberg code (isotropic or anisotropic) to avoid the standard use of the semiempirical parameter μ^*, which adds unnecessary uncertainty to T_c predictions. We evaluate the prediction accuracy of the method by simulating the superconducting properties of a set of layered superconductors, which feature unconventional Coulomb effects: CaC_6, MgB_2, Li-doped β-ZrNCl and YNi_2B_2C. We find that the estimated critical temperatures are consistent with those from *ab-initio* density functional theory for superconductors, and in close agreement with the experimental values.

1. Introduction

Calculations of the critical temperature (T_c) of conventional superconductors are commonly based on Eliashberg theory [1–4]. This is, in principle, a comprehensive theory of the superconducting state, including both electron–phonon and Coulomb effects. The usual application of Eliashberg theory to realistic systems is, however, oversimplified [5] in that the Coulomb interaction is reduced to a single semi-empirical parameter μ^* [4–6]. In recent years the problem of developing a fully *ab-initio* Eliashberg theory accounting for Coulomb and phonon interactions on equal footing has been addressed in detail [7–10]. An extension of the Eliashberg approach to include dynamical Coulomb interactions is computationally very expensive as it involves the evaluation of slowly converging Matsubara frequency summations. Smart summation algorithms for the simulation of real materials have been developed, such as those presented in [9] and [10]. Nevertheless, the computational cost is still very high compared to density functional theory for superconductors (SCDFT) [10, 11] and conventional Eliashberg codes in the μ^* approximation [12].

On the other hand, for most phonon-driven superconductors plasmonic pairing contributions are negligible, and accurate predictions can be obtained by a proper treatment of the static Coulomb interaction [8, 10]. We show that in this case the computationally demanding parts of the Matsubara sums can be evaluated analytically, similarly to how it is done in SCDFT [10, 11, 13–16]. The approach that we present follows the lines of a scheme discussed by Scalapino, Schrieffer and Wilkins [5] and corresponds to the static limit of the hybrid Eliashberg-SCDFT approach by Davydov *et al* [10]. For classic elemental superconductors we do not expect this method to lead to significant differences with respect to the $\mu^* = 0.1$ rule, which was meant to describe these materials [4, 17, 18]. Deviations are foreseen for less common superconductors where Coulomb interactions have a non-trivial behavior, like Chevrel phases [19], multigap superconductors [20, 21] and low dimensional systems. In this work we focus on the application of the method to a set of layered compounds, namely, CaC_6, MgB_2, $Li_{0.5}ZrNCl$ and YNi_2B_2C.

The paper is organized as follows: in section 2 we review the anisotropic Eliashberg theory and discuss our approach for an analytic Matsubara integration of high-energy Coulomb effects (section 2.1). Further simplifications are introduced by employing suitable isotropic approximations (section 2.2). The isotropic

approach is used to estimate the superconducting properties of the chosen set of materials. Results are presented and discussed in section 3.

2. Eliashberg theory with static Coulomb interactions

Eliashberg theory is a many-body Green's-function approach for the description of conventional superconductors, where the pairing is driven by the phonon-induced attraction between the electrons [2–5, 12, 22]. For a recent review of conventional Eliashberg theory and its current extensions we refer the reader to [10]. Here, we use the same notation to summarize the key aspects of the method. Eliashberg theory relies on Migdal's theorem to treat the electron–phonon interaction accurately to order ω_D/E_F, where the phonon energy scale, set by the Debye frequency ω_D, is assumed to be much smaller than the electronic Fermi energy E_F. This amounts to treat the electron self-energy $\bar{\Sigma}(k, i\omega_n)$ up to second order in the electron–phonon coupling. On the contrary, there is no small parameter that allows for a satisfactory perturbative treatment of the Coulomb interaction. The possibility of a plasmon enhancement of T_c is however neglected. The electronic band structure ε_k is assumed to be weakly perturbed by the superconducting condensation and accurately described by normal-state density functional theory [23–25]. Additionally, one has to take into account a static Coulomb interaction $W_{k,k'}$, which opposes the formation of the superconducting state. Under these assumptions, the Eliashberg self-energy is usually expressed in terms of the mass renormalization function $Z(k, i\omega_n)$ and the superconducting order parameter $\phi(k, i\omega_n)$, through its decomposition into Pauli matrices ($\tau_{0,1}$) [10]:

$$\bar{\Sigma}(k, i\omega_n) = i\omega_n [1 - Z(k, i\omega_n)]\,\tau_0 + \phi(k, i\omega_n)\tau_1, \tag{1}$$

where $k = (\boldsymbol{k}, n)$ is a combined momentum and band index and ω_n are fermionic Matsubara frequencies. The problem of calculating $\bar{\Sigma}$ (and ultimately the one-electron Green's function) is then reduced to solving coupled equations for Z and ϕ. These equations are:

$$Z(k, i\omega_n) = 1 + \frac{1}{\beta}\sum_{k',n'} \frac{\lambda_{k,k'}(i\omega_n - i\omega_{n'})}{N(0)} \frac{\omega_{n'} Z(k', i\omega_{n'})}{\omega_n \Theta(k', i\omega_{n'})}, \tag{2}$$

$$\phi^{ph}(k, i\omega_n) = \frac{1}{\beta}\sum_{k',n'} \frac{\lambda_{k,k'}(i\omega_n - i\omega_{n'})}{N(0)} \frac{\phi(k', i\omega_{n'})}{\Theta(k', i\omega_{n'})}, \tag{3}$$

$$\phi^{c}(k) = -\frac{1}{\beta}\sum_{k',n'} W_{k,k'} \frac{\phi(k', i\omega_{n'})}{\Theta(k', i\omega_{n'})}, \tag{4}$$

where we have introduced the function:

$$\Theta(k, i\omega_n) = [\omega_n Z(k, i\omega_n)]^2 + \varepsilon_k^2 + \phi^2(k, i\omega_n), \tag{5}$$

and split $\phi(k, i\omega_n)$ into phonon (ϕ^{ph}) plus Coulomb (ϕ^c) contributions. Note that, since retardation effects in the Coulomb repulsion are disregarded, $\phi^c(k)$ is frequency independent and $Z(k, i\omega_n)$ is entirely determined by the phonon-mediated interaction $\lambda_{k,k'}(i\nu_n)$ [4]. The electron–phonon coupling is usually defined by its spectral representation,

$$\lambda_{k,k'}(i\nu_n) = \int_0^\infty d\omega\, \alpha^2 F_{k,k'}(\omega) \frac{2\omega}{\nu_n^2 + \omega^2}, \tag{6}$$

in terms of the Eliashberg function:

$$\alpha^2 F_{k,k'}(\omega) = N(0) \sum_\nu |g_{kk'\nu}|^2 \delta(\omega - \omega_{\boldsymbol{q}\nu}), \tag{7}$$

where $N(0)$ is the electronic density of states at the Fermi level and $g_{kk'\nu}$ are the electron–phonon matrix elements for the scattering between electronic states k and k' through a phonon with wave vector $\mathbf{q} = \mathbf{k} - \mathbf{k}'$ and branch index ν. $W_{k,k'}$ is given by the matrix elements of the screened Coulomb interaction with respect to the Kohn–Sham orbitals,

$$W_{k,k'} = 4\pi \sum_{\boldsymbol{G},\boldsymbol{G}'} \epsilon^{-1}_{\boldsymbol{G}\boldsymbol{G}'}(\boldsymbol{q}) \times \frac{\langle k'|e^{-i(\boldsymbol{q}+\boldsymbol{G})\cdot\boldsymbol{r}}|k\rangle\langle k|e^{i(\boldsymbol{q}+\boldsymbol{G}')\cdot\boldsymbol{r}}|k'\rangle}{|\boldsymbol{q}+\boldsymbol{G}||\boldsymbol{q}+\boldsymbol{G}'|}, \tag{8}$$

where **G** are reciprocal lattice vectors and the static approximation for the dielectric matrix $\epsilon^{-1}_{\boldsymbol{G}\boldsymbol{G}'}(\boldsymbol{q})$ is made.

2.1. Analytic summation of the Coulomb interaction

Solving the Eliashberg equations becomes computationally affordable if a small cutoff compared to E_F can be introduced in the summations over the Matsubara frequencies. The ω_n sums in equations (2) and (3) converge within an energy scale of the order of a few times ($\sim$ 5 to 10) ω_D, that is the upper characteristic frequency of the electron–phonon spectral function $\alpha^2F_{k,k'}(\omega)$. This enables to set a cutoff Matsubara point ω_{n_c}, above which one can safely assume $Z(k, i\omega_n) = 1$ and $\phi^{ph}(k, i\omega_n) = 0$. Based on this observation, we rewrite equation (4) in the following form:

$$\phi^c(k) = -\frac{1}{\beta}\sum_{k'} W_{k,k'}\left[\sum_{n'=-n_c}^{n_c}\frac{\phi(k', i\omega_{n'})}{\Theta(k', i\omega_{n'})} + \sum_{|n'|>n_c}\frac{\phi^c(k')}{\omega^2_{n'} + \varepsilon^2_{k'} + \phi^{c2}(k')}\right], \tag{9}$$

where the summation for $|\,\omega_{n'}\,| > \omega_{n_c}$ in the second term has been simplified by replacing $Z(k, i\omega_n)$ with unity and $\phi(k, i\omega_n)$ with $\phi^c(k)$. We note that the reduced Matsubara-frequency dependence of the argument allows for a semianalytic evaluation of this sum by using the relation:

$$\frac{1}{\beta}\sum_n \frac{1}{\omega_n^2 + A} = \frac{1}{2}\frac{\tanh\left[\frac{\beta\sqrt{A}}{2}\right]}{\sqrt{A}}. \tag{10}$$

Handling equation (9) by means of equation (10) leads to the expression:

$$\phi^c(k) = -\sum_{k'} W_{k,k'}\left\{\frac{1}{2}\frac{\tanh\left[\frac{1}{2}\beta\sqrt{\varepsilon^2_{k'} + \phi^{c2}(k')}\right]}{\sqrt{\varepsilon^2_{k'} + \phi^{c2}(k')}} + \frac{1}{\beta}\sum_{n'=-n_c}^{n_c}\left[\frac{\phi(k', i\omega_{n'})}{\Theta(k', i\omega_{n'})} - \frac{\phi^c(k')}{\omega^2_{n'} + \varepsilon^2_{k'} + \phi^{c2}(k')}\right]\right\}, \tag{11}$$

where the remaining Matsubara frequency summation is restricted, for both phonon and Coulomb contributions, to a narrow energy window. Equation (11) represents a huge simplification, because it effectively separates the low-energy scale at which the electron–phonon coupling is active, from the high-energy scale associated with Coulomb renormalization effects. Concerning the summation over k', this can be carried out differently depending on the value of $\varepsilon_{k'}$. The integration over low-energy states would benefit from the use of smart interpolation algorithms, such as that developed by R. Margine and coworkers [26–28], which allows for a very fine yet efficient sampling of the electron–phonon scattering processes near the Fermi surface. Less accuracy is needed while integrating over high-energy states, as these essentially contribute via Coulomb effects, which are weakly k-dependent. Hence, the summation over k' can be limited to a sparse set of points, e.g. by means of the energy-dependent random sampling used in SCDFT [13]. Actually, one might even resort to a simplified isotropic treatment of the Coulomb interaction (see section 2.2), justified by the fact that anisotropy effects in $W_{k,k'}$ are expected to average out over a large energy scale.

2.2. Isotropic approximation

Despite the simplifications introduced so far, solving the Eliashberg equations still involves the significant cost of performing a k-integration able to resolve the properties of the electron–phonon coupling near the Fermi surface, and to account for the full extent of the Coulomb interaction. In order to overcome this numerical issue, most Eliashberg codes resort to a simplified approach by neglecting the k-dependence in

both $\lambda_{k,k'}$ and $W_{k,k'}$. For the electron–phonon coupling, the isotropic approximation is defined by averaging equation (7) over the Fermi surface:

$$\alpha^2F(\omega) = \frac{1}{N(0)^2}\sum_{k,k'}\alpha^2F_{k,k'}(\omega)\delta(\varepsilon_k)\delta(\varepsilon_{k'}), \tag{12}$$

which, through equation (6), yields the isotropic kernel $\lambda(i\nu_n)$. Results show that this approximation is quite accurate for the estimation of T_c. In fact, the anisotropy in the electron–phonon coupling turns out to have no relevant effect on T_c for the majority of bulk superconductors, possibly being truly essential only to describe MgB_2 [29–31]. On the other hand, it affects, often crucially, all those superconducting properties which depend on the excitation spectrum (such as tunneling behavior, thermodynamic properties and magnetic response) [32–34].

Handling the k-dependence of the Coulomb interaction is a more subtle problem. Formally, this dependence cannot be simply neglected because the integration in equation (4) would diverge logarithmically. For this reason the μ^* approach, which involves the isotropic approximation, relies on the introduction of an arbitrary high-energy cutoff (usually chosen as E_F) [4, 5, 35, 36]. The most sensible strategy [8, 10, 31] is to approximate $W_{k,k'}$ by its average over surfaces of constant energy (ε) in k-space, i.e.:

$$W(\varepsilon,\varepsilon') = \frac{1}{N(\varepsilon)N(\varepsilon')}\sum_{k,k'}W_{k,k'}\delta(\varepsilon_k-\varepsilon)\delta(\varepsilon_{k'}-\varepsilon'), \tag{13}$$

where $N(\varepsilon) = \sum_k \delta(\varepsilon_k - \varepsilon)$. By averaging over k equations (2), (3) and (11), we obtain the following isotropic Eliashberg equations:

$$Z(i\omega_n) = 1 + \frac{\pi}{\beta}\sum_{n'=-n_c}^{n_c}\frac{\lambda(i\omega_n - i\omega_{n'})\omega_{n'}Z(i\omega_{n'})}{\omega_n\sqrt{[\omega_{n'}Z(i\omega_{n'})]^2 + \phi^2(0,i\omega_{n'})}}, \tag{14}$$

$$\phi^{ph}(i\omega_n) = \frac{\pi}{\beta}\sum_{n'=-n_c}^{n_c}\frac{\lambda(i\omega_n - i\omega_{n'})\phi(0,i\omega_{n'})}{\sqrt{[\omega_{n'}Z(i\omega_{n'})]^2 + \phi^2(0,i\omega_{n'})}}, \tag{15}$$

$$\phi^c(\varepsilon) = -\int d\varepsilon' W(\varepsilon,\varepsilon')N(\varepsilon')\left\{\frac{1}{2}\frac{\tanh\left[\frac{\beta}{2}\sqrt{\varepsilon'^2+\phi^{c2}(\varepsilon')}\right]}{\sqrt{\varepsilon'^2+\phi^{c2}(\varepsilon')}} + \frac{1}{\beta}\sum_{n'=-n_c}^{n_c}\left[\frac{\phi(\varepsilon',i\omega_{n'})}{\Theta(\varepsilon',i\omega_{n'})} - \frac{\phi^c(\varepsilon')}{\omega_n^2+\varepsilon'^2+\phi^{c2}(\varepsilon')}\right]\right\}, \tag{16}$$

where

$$\phi(\varepsilon,i\omega_n) = \phi^{ph}(i\omega_n) + \phi^c(\varepsilon), \tag{17}$$

and

$$\Theta(\varepsilon,i\omega_n) = [\omega_n Z(i\omega_n)]^2 + \varepsilon^2 + \phi^2(\varepsilon,i\omega_n). \tag{18}$$

The resulting scheme is formally similar to the static limit of the hybrid SCDFT-Eliashberg method recently introduced in [10]. The main difference lies in equations (14) and (15), where the energy dependence of $\phi^c(\varepsilon)$ and $N(\varepsilon)$ has been neglected to allow for an analytic integration over ε, as in usual applications of conventional Eliashberg theory [4]. For the numerical tests discussed in section 3 we solve equations (14)–(18), with the only exception of MgB_2, for which we use a 2-band generalization [37].

3. Superconducting properties of layered compounds within ab-initio Eliashberg theory

For most conventional superconductors the role of Coulomb interactions is almost trivial, as it is reduced to a scaling of the superconducting gap at the Fermi energy. This is due to the fact that by integrating $W(\varepsilon,\varepsilon')$ over a large energy scale, specific material properties are often washed out and the resulting effect is nearly material independent. The striking evidence for this is that the McMillan formula for T_c, which depends on the single Coulomb parameter μ^*, works reasonably well for many materials, with the only caveat that $\mu^* \simeq 0.1$ should be used for sp-electron systems and $\mu^* \simeq 0.14$ for d-electron systems [4, 36]. However,

peculiarities in the electronic band structure may lead to significant exceptions. An interesting case recently discussed are Chevrel phases, where the band character changes abruptly close to the Fermi level, significantly weakening the Coulomb renormalization [19], and for which a naive application of the McMillan formula gives a T_c more than 50% larger than the experimental value. Anomalous Coulomb effects are likely to occur when the Fermi level is close to Van Hove singularities causing $W(\varepsilon, \varepsilon')$ to suddenly drop or increase. A typical example is the proximity of the Fermi level to a band gap, as in weakly doped insulators [48, 49], or to a sharp peak in the density of state, like in high pressure sulphur hydride [7, 50]. From purely theoretical arguments, an enhancement of Coulomb interactions is more likely to occur in low dimensional systems, because of the reduced metallic screening [51]. In this work we test our method on four layered systems, which have been formerly investigated within SCDFT [16, 21, 31, 34, 38, 52, 53]. The coupling parameters used in the calculations are collected in table 1: electron–phonon couplings are taken from the literature [31, 38, 39], while the Coulomb interaction W is computed within the RPA approximation using the Elk code [54].

3.1. CaC_6

CaC_6 is an intercalated graphite compound with an experimental critical temperature of 11.5 K [40]. Superconductivity arises from the strong electron–phonon coupling provided by both C and Ca phonon modes [55]. This coupling is strongly anisotropic with C- and Ca-related phonons acting selectively on the multiple Fermi surface sheets of the system [22, 56]. This leads to a strong anisotropy of the superconducting gap [34], but has a rather small effect on T_c (of the order of 1 K). The μ^* approach to the Coulomb interaction is relatively accurate, although a $\mu^* = 0.14$ needs to be used in order to reproduce the experimental T_c, whereas the conventional value of 0.1 yields an overestimation of 40%.

By solving equations (14)–(18) using the *ab-initio* calculated couplings of figures 1(a)–(d), we obtain an excellent T_c estimate of 10.7 K. This value is essentially identical to that provided by SCDFT and the full-scale Eliashberg equations of [10]. The unusually strong Coulomb renormalization effect is due to the block-matrix structure of the screened Coulomb interaction $W(\varepsilon, \varepsilon')$, which effectively restricts the Coulomb renormalization to a 5 eV energy window [56], instead of employing the full valence bandwidth of 20 eV. This block structure is clearly visible in figure 1(b).

3.2. MgB_2

MgB_2 is probably the most remarkable phononic superconductor. It has a T_c of 39 K and the unique feature of two, electronically well-distinguished superconducting gaps. The highest gap occurs in the hole-doped strongly covalent σ bands, while the lowest gap arises from the π bands of the B electrons. Electronic [57, 58] and phononic [59–61] properties of this material have been discussed in detail in a number of excellent theoretical studies. Due to the different nature of σ and π states crossing the Fermi level, the Coulomb interaction acts differently on the two bands. Both states contribute significantly to metallic screening [20, 21], however, electrons in the more spatially constrained σ states feel a 30% stronger Coulomb repulsion. The most simplified approach to MgB_2 needs to account for this two-band anisotropic structure in both the electron–phonon coupling and the screened Coulomb repulsion. Solving the Eliashberg equations with the coupling functions shown in figures 1(f)–(p), we obtain a T_c of 33.5 K, which is about 15% smaller than the experimental value. A similar underestimation resulted from previous SCDFT calculations [31]. We note that such an error in the predicted T_c by means of *ab-initio* methods is relatively common, and overall quite good, owing to the number of approximations involved. In the present case this underestimation is probably related to some inaccuracy in the calculated electron–phonon coupling. In fact, the average coupling that we compute ($\lambda = 0.7$) turns out to be smaller than that provided by a likely more accurate Wannier-function approach [62].

3.3. YNi_2B_2C

The next system in our set is the quaternary borocarbide YNi_2B_2C, whose crystal structure is shown in figure 1(o). The peculiarity of this material is the pinning of the Fermi energy to a Van Hove singularity, which leads to an extremely sharp peak (less than 100 meV wide) in the density of states (figure 1(n)). This unique feature of YNi_2B_2C challenges the validity of the adiabatic approximation [1], the neglect of dynamical Coulomb effects [10, 53], and the use of an energy independent electron–phonon coupling. Nevertheless, we have tested our approach on this system. The first problem that one encounters is the choice of the lattice parameters. Most *ab-initio* simulations are either carried out at the *ab-initio* relaxed lattice (typically in the local or semi-local density approximation [25]) or at the experimental lattice. Usually, the latter approach is slightly more accurate, but results do not depend critically on the choice. However, it turns out that for YNi_2B_2C this is not the case. By simulating the system at the experimental lattice we obtain an integrated electron–phonon coupling $\lambda = 0.86$, whereas using the LDA relaxed lattice gives $\lambda = 0.56$, that is a

Table 1. Material parameters and estimated critical temperatures and superconducting gaps. λ is the averaged electron–phonon coupling. ω_{log} is the logarithmic average of the α^2F function [4], in meV. $N(0)$ is the density of states at the Fermi level, in states/eV/cell/spin. $\mu = W(0,0)N(0)$ is the Coulomb potential at the Fermi level. T_c, T_c^{McM} and T_c^{exp} are, respectively, the critical temperature computed from equations (14)–(18), the McMillan critical temperature evaluated at $\mu^* = 0.1$, and the experimental critical temperature, in K. Δ and Δ^{exp} are, respectively, the superconducting gap values predicted from equations (14)–(18) and the experimental gaps at $T = 0$, in meV.

		λ	$\omega_{\log}$	$N(0)$	μ	T_c	T_c^{McM}	T_c^{exp}	Δ	Δ^{exp}
CaC_6		0.78 [31]	30.0 [31]	0.73	0.27	10.7	16.1	11.5 [40]	1.72	1.6 [41]
MgB_2	σ	0.812 [31]	60.8 [31]	0.145	0.19				6.09	7.2 [43]
	π	0.267 [31]	56.7 [31]	0.191	0.19	33.5	26.6	39 [42]	2.17	2.8 [43]
	$\sigma - \pi$	0.199 [31]	51.3 [31]	—	0.07				—	—
YNi_2B_2C		0.86	23.4	1.92	0.33	11.3	15.2	14.6 [44]–15.6 [45]	1.74	1.8 [44]–1.92 [46]
$Li_{0.5}ZrNCl$		0.97 [38]	27.0 [38]	1.24	0.54	9.5	22.4	$\simeq$11 [47]	1.38	—

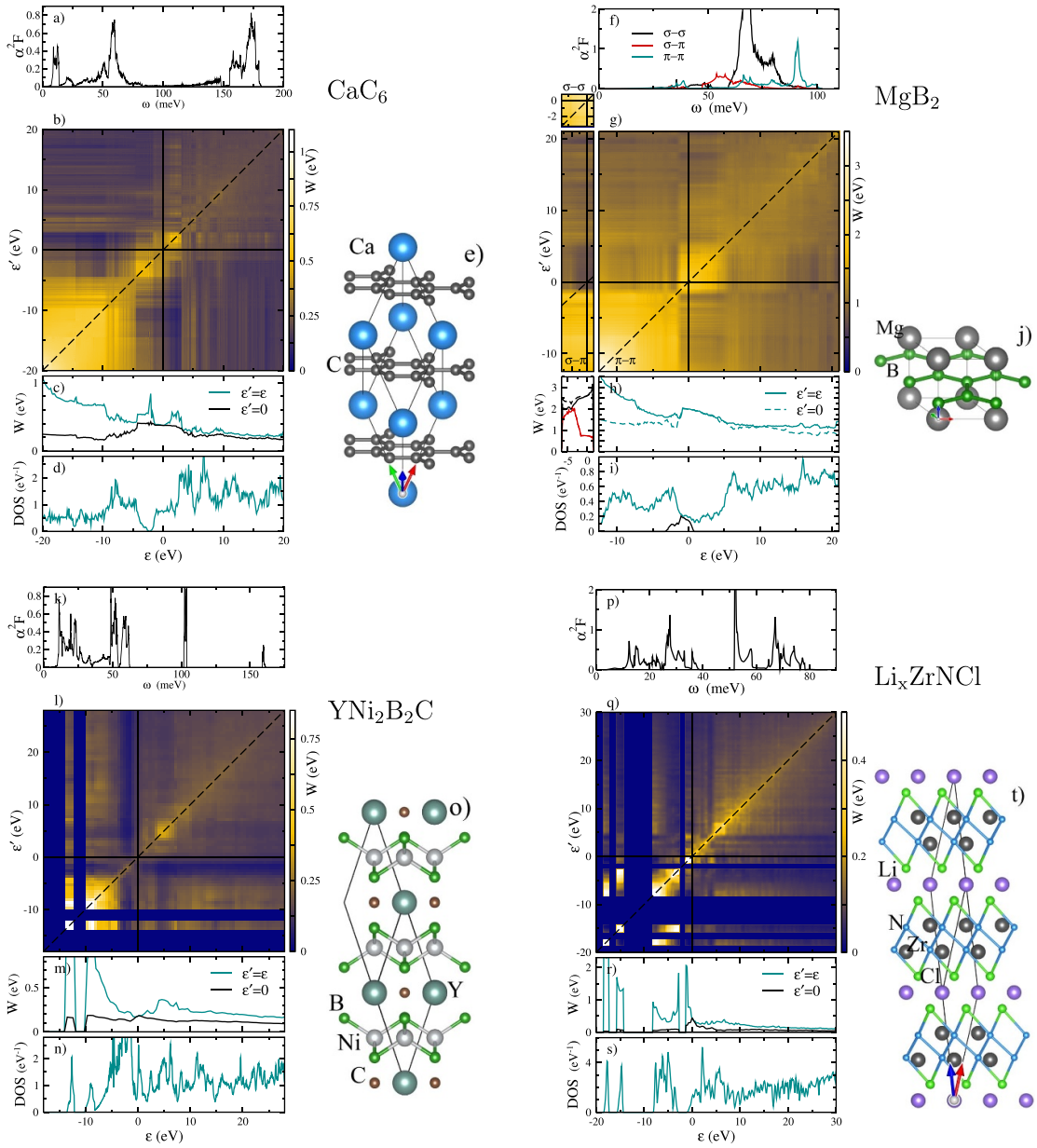

Figure 1. Couplings and crystal structures of the layered systems: CaC_6 ((a)–(e)), MgB_2 ((f)–(j)), YNi_2B_2C ((k)–(o)) and $Li_{0.5}ZrNCl$ ((p)–(t)). Panels (a),(f),(k),(p): α^2F electron–phonon function [31, 38, 39]. Panels (b),(g),(l),(q): Coulomb function $W(\varepsilon,\varepsilon')$; a diagonal cut ($\varepsilon=\varepsilon'$) and a Fermi surface cut ($\varepsilon'=0$) of $W(\varepsilon,\varepsilon')$ are displayed in panels (c),(h),(m),(r). Panels (d),(i),(n),(s): electronic density of states per unit cell. Crystal structures are sketched in panels (e),(j),(o),(t).

large discrepancy. We do not delve here into this complex issue, and choose to use the electron–phonon coupling computed at the experimental lattice (shown in figure 1(o)), as it best describes the vibrational spectrum [39, 63, 64]. Consistently, we compute the static screened Coulomb interaction with the same structure. As shown in figures 1(l) and (m) the Coulomb repulsion is relatively smooth, with decreasing matrix elements at higher energies, not unlike the electron gas model [65]. However, since $W(\varepsilon,\varepsilon')$ enters equation (16) jointly with the density of states, it plays a non trivial role in determining T_c. We obtain a T_c of 11.3 K, which underestimates the experimental value, reported to be within the range 14.6 K [44]–15.6 K [45]. A simple McMillan estimation with $\mu^*=0.1$ predicts a T_c of 15.2 K, in better agreement with experiments, even though, due to the d character of the density of states at the Fermi level, a larger μ^* is conventionally recommended [4].

3.4. $Li_{0.5}ZrNCl$

Lastly, we consider the lithium-doped ternary transition-metal nitride halide ZrNCl. Undoped ZrNCl is a layered semiconductor. The intercalation of lithium impurities into the Van der Waals gap (the interlayer space) leads, for $x=0.5$, to the crystal structure shown in figure 1(t). This material has been studied

thoroughly by Akashi and coworkers [38] within the SCDFT framework. Here, we use the electron–phonon coupling extracted from their reference and shown in figure 1(p).

The Coulomb interaction matrix that we computed is shown in figures 1(q) and (r). Compared to MgB_2 and CaC_6, this function is significantly more structured, owing to the fact that, this system being a doped insulator, the metallic screening is poor. In fact at the band edges (that is close to the points where the density of states tends to zero in figure 1(r)), $W(\varepsilon,\varepsilon')$ shows very high peaks caused by the $1/q$ divergence of the bare Coulomb interaction. Since the Fermi level is very close to one of the peaks, the Coulomb repulsion is strong. A $\mu^* = 0.2$ is required in the McMillan formula to reproduce the extrapolated experimental [47] T_c of approximately 11 K, whereas the standard $\mu^* = 0.1$–0.14 gives a T_c in the range 18–22 K, that is almost twice the experimental value. On the contrary, our Eliashberg approach yields an excellent T_c estimate of 9.5 K. However, one should point out that due to the peaked-structure of $W(\varepsilon,\varepsilon')$, the estimation of T_c is very sensitive to parameters like the position of the Fermi level and properties of the dielectric function. Therefore, in a doped insulator of this kind, a 20% error in T_c is usually expected [48]. As a test, we have used the same input functions to compute the critical temperature within SCDFT. This latter approach gives a T_c of 13.1 K, that is about 15% higher than the experimental value. We observe that previous SCDFT-based calculations on this system [38] predicted a very low T_c, highlighting a large discrepancy between theory and experiments. We can now assert that the problem had to be ascribed to inaccuracy of the functional available at the time [11].

4. Conclusions

We have presented a minimal yet efficient approach to include static Coulomb interactions in Eliashberg theory from first principles, which avoids the arbitrariness introduced by the use of the adjustable parameter μ^*. The method is formally equivalent to the static limit of the *ab-initio* Eliashberg theory recently proposed in [10], but, unlike the more complex original scheme, allows for a straightforward implementation in conventional Eliashberg codes. In the derived equations, the effects of the Coulomb interaction outside the phonon frequency range are evaluated analytically, and the numerical integration is reduced, as for the standard approach, to the energy window $0 \rightarrow \omega_{n_c} \sim 10\,\omega_D$. Both parts include the matrix elements of the screened Coulomb interaction, which can be computed using the random phase approximation for the dielectric matrix. In practice, this is the main additional computational step compared to conventional implementations. We have tested our method on the layered superconducting materials CaC_6, MgB_2, YNi_2B_2C and Li-doped β-ZrNCl, which present a non-monotonous behavior of the Coulomb repulsion, such to challenge the validity of the μ^* approximation. The new approach turns out to be accurate as the estimated critical temperatures are consistent with SCDFT values. The agreement with experiments is excellent in terms of both T_c's and gaps for CaC_6, MgB_2 and Li-doped β-ZrNCl, with a significant improvement in prediction quality with respect to the μ^* formula. We observe, however, a large error (25%) in the predicted T_c of YNi_2B_2C. We believe that this anomaly should be further investigated, as it stems from a difficulty in determining the electron–phonon coupling, and might point to strong non-adiabatic effects related to the presence of a sharp Van Hove singularity at the Fermi level.

Data availability statement

All data that support the findings of this study are included within the article (and any supplementary files).

Acknowledgment

CP acknowledges financial support by the CarESS project.

ORCID iDs

Camilla Pellegrini https://orcid.org/0000-0003-2614-1111
Antonio Sanna https://orcid.org/0000-0001-6114-9552

References

[1] Migdal A B 1958 *Sov. Phys. JETP* **7** 996
[2] Eliashberg G 1960 *J. Exp. Theor. Phys.* **38** 966; Eliashberg G 1960 *Sov. Phys. JETP* **11** 696
[3] Vonsovsky S, Izyumov Y, Kurmaev E, Brandt E and Zavarnitsyn A 1982 *Superconductivity of Transition Metals: Their Alloys and Compounds (Springer Series in Solid-State Sciences Series)* (Berlin: Springer)

[4] Allen P B and Mitrović B 1983 *Theory of Superconducting Tc (Solid State Physics)* vol 37, ed F S Henry Ehrenreich and D Turnbull (New York: Academic) pp 1–92
[5] Scalapino D J, Schrieffer J R and Wilkins J W 1966 *Phys. Rev.* **148** 263
[6] Morel P and Anderson P W 1962 *Phys. Rev.* **125** 1263
[7] Sano W, Koretsune T, Tadano T, Akashi R and Arita R 2016 *Phys. Rev.* B **93** 094525
[8] Sanna A, Flores-Livas J A, Davydov A, Profeta G, Dewhurst K, Sharma S and Gross E K U 2018 *J. Phys. Soc. Japan* **87** 041012
[9] Wang T, Nomoto T, Nomura Y, Shinaoka H, Otsuki J, Koretsune T and Arita R 2020 *Phys. Rev.* B **102** 134503
[10] Davydov A, Sanna A, Pellegrini C, Dewhurst J K, Sharma S and Gross E K U 2020 *Phys. Rev.* B **102** 214508
[11] Lüders M, Marques M A L, Lathiotakis N N, Floris A, Profeta G, Fast L, Continenza A, Massidda S and Gross E K U 2005 *Phys. Rev.* B **72** 024545
[12] Ummarino G A C 2013 *Emergent Phenomena in Correlated Matter* ed E Pavarini, E Koch and U Schollwöck (Jülich: Verlag des Forschungszentrum Jülich) ch 13, p 395
[13] Marques M A L, Lüders M, Lathiotakis N N, Profeta G, Floris A, Fast L, Continenza A, Gross E K U and Massidda S 2005 *Phys. Rev.* B **72** 024546
[14] Akashi R and Arita R 2013 *Phys. Rev. Lett.* **111** 057006
[15] Akashi R and Arita R 2014 *J. Phys. Soc. Japan* **83** 061016
[16] Massidda S *et al* 2009 *Supercond. Sci. Technol.* **22** 034006
[17] McMillan W L 1968 *Phys. Rev.* **167** 331
[18] Allen P B and Dynes R C 1975 *Phys. Rev.* B **12** 905
[19] Marini G, Sanna A, Pellegrini C, Bersier C, Tosatti E and Profeta G 2021 *Phys. Rev.* B **103** 144507
[20] Floris A, Profeta G, Lathiotakis N N, Lüders M, Marques M A L, Franchini C, Gross E K U, Continenza A and Massidda S 2005 *Phys. Rev. Lett.* **94** 037004
[21] Floris A *et al* 2007 *Phys. C: Supercond. Appl.* **456** 45
[22] Sanna A, Pittalis S, Dewhurst J K, Monni M, Sharma S, Ummarino G, Massidda S and Gross E K U 2012 *Phys. Rev.* B **85** 184514
[23] Hohenberg P and Kohn W 1964 *Phys. Rev.* **136** B864
[24] Kohn W and Sham L J 1965 *Phys. Rev.* **140** A1133
[25] Dreizler R and Gross E K U 1990 *Density Functional Theory—An Approach to the Quantum Many-Body Problem* (Berlin: Springer)
[26] Margine E R and Giustino F 2013 *Phys. Rev.* B **87** 024505
[27] Poncé S, Margine E, Verdi C and Giustino F 2016 *Comput. Phys. Commun.* **209** 116
[28] Boeri L *et al* 2021 *J. Phys.: Condens. Matter.* **34** 183002
[29] Kong Y, Dolgov O V, Jepsen O and Andersen O K 2001 *Phys. Rev.* B **64** 020501
[30] Liu A Y, Mazin I I and Kortus J 2001 *Phys. Rev. Lett.* **87** 087005
[31] Sanna A, Pellegrini C and Gross E K U 2020 *Phys. Rev. Lett.* **125** 057001
[32] Floris A, Sanna A, Massidda S and Gross E K U 2007 *Phys. Rev.* B **75** 054508
[33] Heil C, Poncé S, Lambert H, Schlipf M, Margine E R and Giustino F 2017 *Phys. Rev. Lett.* **119** 087003
[34] Gonnelli R S *et al* 2008 *Phys. Rev. Lett.* **100** 207004
[35] Morel P and Anderson P W 1962 *Phys. Rev.* **125** 1263
[36] Flores-Livas J A, Boeri L, Sanna A, Profeta G, Arita R and Eremets M 2020 *Phys. Rep.* **856** 1
[37] In this case the Fermi surface quantities are resolved in σ, π band components similarly to [20, 31].
[38] Akashi R, Nakamura K, Arita R and Imada M 2012 *Phys. Rev.* B **86** 054513
[39] Reichardt W, Heid R and Bohnen K P 2005 *J. Supercond.* **18** 759
[40] Weller T E, Ellerby M, Saxena S S, Smith R P and Skipper N T 2005 *Nat. Phys.* **1** 39
[41] Bergeal N *et al* 2006 *Phys. Rev. Lett.* **97** 077003
[42] Nagamatsu J, Nakagawa N, Muranaka T, Zenitani Y and Akimitsu J 2001 *Nature* **410** 63
[43] Heitmann T W *et al* 2004 *Supercond. Sci. Technol.* **17** 237
[44] Raychaudhuri P, Jaiswal-Nagar D, Sheet G, Ramakrishnan S and Takeya H 2004 *Phys. Rev. Lett.* **93** 156802
[45] Cava R J *et al* 1994 *Nature* **367** 252
[46] Ekino T, Fujii H, Kosugi M, Zenitani Y and Akimitsu J 1994 *Phys. C: Supercond.* **235-240** 2529
[47] Taguchi Y, Kitora A and Iwasa Y 2006 *Phys. Rev. Lett.* **97** 107001
[48] Pellegrini C, Glawe H and Sanna A 2019 *Phys. Rev. Mater.* **3** 064804
[49] Sanna A, Davydov A, Dewhurst J K, Sharma S and Flores-Livas J A 2018 *Eur. Phys. J.* B **91** 177
[50] Flores-Livas J A, Sanna A and Gross E 2016 *Eur. Phys. J.* B **89** 63
[51] Giuliani G and Vignale G 2005 *Quantum Theory of the Electron Liquid* (Cambridge: Cambridge University Press)
[52] Sanna A, Profeta G, Floris A, Marini A, Gross E K U and Massidda S 2007 *Phys. Rev.* B **75** 020511
[53] Kawamura M, Akashi R and Tsuneyuki S 2017 *Phys. Rev.* B **95** 054506
[54] The Elk FP-LAPW Code (available at: http://elk.sourceforge.net)
[55] Calandra M and Mauri F 2005 *Phys. Rev. Lett.* **95** 237002
[56] Sanna A, Profeta G, Floris A, Marini A, Gross E K U and Massidda S 2007 *Phys. Rev.* B **75** 020511
[57] An J M and Pickett W E 2001 *Phys. Rev. Lett.* **86** 4366
[58] Kortus J, Mazin I I, Belashchenko K D, Antropov V P and Boyer L L 2001 *Phys. Rev. Lett.* **86** 4656
[59] Bohnen K-P, Heid R and Renker B 2001 *Phys. Rev. Lett.* **86** 5771
[60] Calandra M, Lazzeri M and Mauri F 2007 *Phys. C: Supercond.* **456** 38
[61] Calandra M and Mauri F 2005b *Phys. Rev.* B **71** 064501
[62] Calandra M, Profeta G and Mauri F 2010 *Phys. Rev.* B **82** 165111
[63] Weber F, Pintschovius L, Reichardt W, Heid R, Bohnen K-P, Kreyssig A, Reznik D and Hradil K 2014 *Phys. Rev.* B **89** 104503
[64] Weber F *et al* 2012 *Phys. Rev. Lett.* **109** 057001
[65] Sham L J and Kohn W 1966 *Phys. Rev.* **145** 561